Synthesis of (S)-omeprazole catalyzed by soybean pod peroxidase in water-in-oil microemulsions: optimization and modeling

Yuanyuan Zhang [a,b*] , Hui Tang [a ,b 1], Yashan Deng[d], Depeng Li[a,c], Zhiyong Wang[c,d], Huiling Li[d], Xin Gao[a,c*], Fanye Wang[*]

a State Key Laboratory Base for Eco-Chemical Engineering in College of Chemical Engineering, Qingdao University of Science and Technology, Mail box 70, 53 Zhengzhou Road, Qingdao 266042, China

b William G. Lowrie Department of Chemical and Biomolecular Engineering, The Ohio State University, 151 West Woodruff Avenue, Columbus, Ohio 43210,USA

c Kekulé-Institut für Organische Chemie und Biochemieder Rheinischen Friedrich -Wilhelms-Universität Bonn Gerhard-Domagk-Str. 153121 Bonn Germany

d Department of Pharmaceutical Engineering, College of Chemical Engineering, Qingdao University of Science and Technology, Mail box 70, 53 Zhengzhou Road, Qingdao 266042, China

Abstract

Response surface methodology (RSM) was used to optimize the oxidation of the omeprazole sulfide to (S)-omeprazole catalyzed by environmentally friendly catalyst soybean pod peroxidase (SPP) in cetyltrimethylammonium bromide (CTAB)/isooctane/n-butyl alcohol/water water-in-oil microemulsions. With the initial concentration of SPP of 3200 U ml^{-1}, the conversion of the omeprazole sulfide, the (S)-omeprazole yield and ee were 93.75%, 91.56% and 96.08%, respectively, under the optimal conditions: Wo of 15.85, the concentration of H_2O_2 of 22.44 mM and reaction temperature of 49.68 ℃, respectively. The proposed mechanism of asymmetric sulfoxidations catalyzed by SPP involves three concomitant mechanisms as follows: (1) a two-electron reduction of SPP-I, (2) a single-electron transfer to SPP-I and (3) nonenzymatic reactions, including five enzymatic and two nonenzymatic reactions, which is reasonable and can express the oxidations. With 5.44% of the average relative error, a kinetic model based on the mechanisms fitting observed data very well was established, and the SPP-catalyzed reactions including both the two-electron reduction and the single-electron transfer mechanisms obey ping-pong mechanism with substrate and product inhibition，while nonenzymatic reactions follow a power law. This study has also demonstrated the feasibility of SPP as a substitute with low cost, excellent enantioselectivity and better thermal stability.

[*]*Corresponding author at: Department of Pharmaceutics, Qingdao University of Science and Technology, 53 Zhengzhou Road, 266042 Qingdao, China.
1 The author contributed equally to this work and should be considered co-first authors.
E-mail address: zyy800928@126.com (Y.Zhang); 523985377@qq.com (X. Gao); zljh06@163.com (J.Liu); fywang8209@163.com (F Wang)

1 INTRODUCTION

Proton pump inhibitors (PPIs), one of chiral sulfoxides, are a class of effective drugs for the treatment

of ulcerative diseases of the digestive system. Chiral sulfoxides are mainly synthesized by chemical

oxidizing (Delamare et al., 2009; Federsel,; Prasad, 2001) which has many disadvantages, especially

the unfriendliness to the environment.(Adam et al., 1998; Dembitsky, 2003) Enzymatic oxidation of

prochiral sulfides has been used to prepared chiral sulfoxides due to the enantioselectivity and

regioselectivity of enzyme and mild conditions, which has received considerable attention in the past

few years.(Thomas et al., 2002) Chiral sulfoxides are valuable pharmaceutical compounds, and

asymmetric oxidation of thioethers catalyzed by peroxidases is a hot topic for synthesis.(Carreño,

1995) Some peroxidases, including those from horseradish peroxidase (HRP),(Colonna et al., 1992a;

Harris et al., 1993) soybean peroxidase (SHP),(Blee and Schuber, 1989) *C. fumago*

chloroperoxidase(Colonna et al., 1990; Colonna et al., 1992b; Van Deurzen et al., 1997) and others are

used for asymmetric sulfoxidation with mainly focusing on reaction mechanisms.(Colonna et al.,;

Colonna et al., 1995; Miller et al., 1992; van de Velde et al., 2000) Monoenzyme,(Kamerbeek et al.,; Li

et al.,; Zambianchi et al., 2007; Zhang et al., 2018; Zhang et al., 2019a) and nonenzymatic hemoglobin

myoglobin (Ozaki et al.,; Ozaki et al., 1999) and cytochrome (Akasaka et al.,) have been found to

catalyze asymmetric oxidations, however, there are some serious disadvantages, such as the need for

expensive cofactors or cofactor recycling systems, or the use of expensive and less commercial sources

of enzymes.

For years, extensive research has been carried out on the mechanism oxidation catalyzed by

peroxidase, and there are two main mechanisms according to the modes of oxygen transfer:(Blee and

Schuber, 1989; Doerge, 1986; Kobayashi et al., 1987; Ortiz de Montellano, 1987; Singh et al., 2012;

Watanabe et al., 1980)

(1) a two-electron reduction mechanism involving a two-electron reaction, involving reactions 1

and 2,

$$E + A \longrightarrow E_1 + Q \qquad (1)$$

$$E_1 + B \longrightarrow \begin{array}{l} E + P_S \\ \\ E + P_R \end{array} \qquad (2)$$
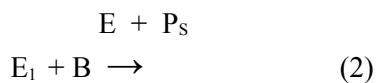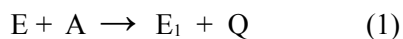
(2) a single-electron transfer mechanism consisting of reactions 1, 3 and 4,

$$E_1 + B \longrightarrow E_2 + C \qquad (3)$$

$$E_2 + C \longrightarrow \begin{array}{l} E + P_S \\ \\ E + P_R \end{array} \qquad (4)$$
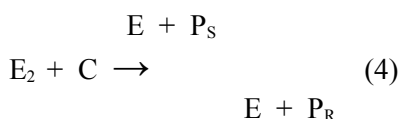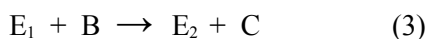
Several simple kinetic models have been established.(Hong et al., 2008; Lee et al., 2007; Perez and Dunford, 1990; Singh et al., 2012) However, more exploration should be performed to identify the reaction mechanism further, and the establishment of a kinetic model can well help to comprehend the mechanism. In this study, soybean pods peroxidase (SPP) extracted from soybean pods was employed for asymmetric sulfoxidation of thioether to chiral sulfoxide for the first time. SPP is a cheap, widely available and environmentally friendly catalyst, and is different from SHP which is from the seed coat. As far as we know, SPP has not been used in asymmetric oxidation yet.

Enzyme could be expected to have superactivity in microemulsions which are very favorable for hydrophobic substrates,(Lopez et al.,; Lopez et al., 2004; Lopez et al., 2014), thus in the study, the asymmetric sulfoxidation was conducted in water-in-oil microemulsions owing to the hydrophobicity of both substrates and products. For the enzyme catalyzed asymmetric oxidation, there are many factors that affect the conversion and enantiomeric purity of products, such as reaction temperature, Wo(water/isooctane, mol), substrate concentration, etc. In order to decrease the number of experiments, response surface methodology (RSM) was used in the experimental design.

In the study, SPP was extracted from soybean pods, separated and purified to yield SPP which was employed as a biocatalyst for enzymatic oxidations of the omeprazole thioether to form chiral sulfoxide (S)-omeprazole, (S)-enantiomer of omeprazole, in cetyltrimethylammonium bromide (CTAB)/n-hexanol/isooctane. To improve the yield of (S)-omeprazole, the conditions of asymmetric sulfoxidations were optimized using RSM. A kinetic model was established and a reaction mechanism was proposed.

2. EXPERIMENTAL SECTION

2.1 Generals

K$_2$HPO$_4$, citric acid, PEG4000, hydrogen peroxide, anhydrous ethanol, sodium hydroxide, cetyltrimethylammonium bromide (CTAB), hydrogen peroxide (30%), n-butyl alcohol, isooctane and methanol were purchased from Sinopharm Group Chemical Reagent Co., Ltd., respectively, and all the above reagents were of analytical purity and were used directly without further purification. The omeprazole thioether was purchased from Jinan ward Chemical Co., Ltd., (S)-omeprazole from Suzhou Vita Chemical Co., Ltd., omeprazole from Shandong Shouguang Fukang Pharmaceutical Co., Ltd and fresh soybean pods from an urban supermarket of farm produce, respectively. Both the ^{1}H and ^{13}C NMR spectra were recorded in CDCl3 on Bruker AV-500, 500 MHz for ^{1}H and 125 MHz for ^{13}C, respectively, in which CHCl$_3$ was used as internal standard (^{1}H NMR: 7.26 ppm; ^{13}C NMR: 77.36 ppm).

2.2 Isolation and purification of soybean pod peroxidase

Fresh soybean pods (SPs) were cleaned and homogenized at 15000 rpm using a high-speed food mixer, and the homogenized SPs were extracted by phosphate buffer at 4 ℃ for 2h, and then filtered with a 500-mesh filter cloth. The filtrate was then fractionated and purified by a series of operations: impurities removal by zinc ion, fractionation with aqueous two-phase system (PEG 4000, 12%, v/v / K$_2$HPO$_4$, 13%, v/v), ultrafiltration, Sephadex G-75and DEAE chromate graphies, respectively. Finally, the resulted concentrated extract was lyophilized to yield the peroxidase powder with 160 U mg^{-1}.

2.3 Peroxidase-catalyzed sulfoxidation of omeprazole sulfide in water-in-oil microemulsions to prepare (S)-omeprazole

SPP-catalyzed oxidation of the omeprazole sulfide was carried out in water-in-oil microemulsions in 20 ml flask. The CTAB/isooctane/n-butyl alcohol/water water-in-oil microemulsion with Wo of 16 was made up by addition of the amounts of CTAB (1.265g), isooctane (7.8ml), n-butanol (1.2ml), the omeprazole sulfide, totaling 1ml of phosphate buffer solution (pH 7.6) and a stock solution of peroxidase, respectively, which yielded a range of final concentration of peroxidase from 240-3200 U ml^{-1}. The sulfoxidation was initiated by addition of H$_2$O$_2$ into the microemulsion which was placed in a oscillator at 150 rpm and 50 ℃ for 5 h. The enantioselectivity of products and the conversion of the omeprazole sulfide were assayed by HPLC, and sampled using a syringe from the reaction media. To separate the aqueous phase from organic phase, 3-fold distilled water was added into the samples and the organic phase was withdrawn for HPLC assay. The concentration of H$_2$O$_2$ which was sampled

directly from the reaction mixture was assayed by HPLC. The sulfoxidation was terminated by adding 3-fold distilled water into reaction solution, and phase separation was performed using a centrifuge at 4000 rpm to obtain organic and aqueous phase respectively. The latter was extracted with ethyl acetate and then the resulted ethyl acetate layer was combined with the organic phase. The organic phase was used for HPLC assay to determine the enantioselectivity and the conversion. Both the ^{1}H and ^{13}C NMR data obtained for (S)-omeprazole agree with the literature values.(Seenivasaperumal et al., 2010)

2.4 HPLC analysis

The conversion of the omeprazole thioether, the yield of omeprazoles of both S and R configuration were assayed by a chiral HPLC system with an Agilent 1200 LC with a DAD detector working at 302 nm and the column temperature was 30 °C, equipping with a chiral column Amylose-SA (250 × 4.6mm, 5um, YMC, Japan). The enantiomeric excess (ee) was calculated based on the yield of S and R enantiomer. The sample volume was 20 μL (quantitative ring) and the mobile phase was a 15:85 v/v mixture of acetonitrile and phosphate buffer (pH 6.0) at a flow rate of 0.6 mL min^{-1}. The concentration of H_2O_2 was assayed using HPLC with an Inertsil ODS-SP column (150 × 4.6mm, 5μm). The mobile phase was a 2:8 v/v mixtures of methanol and water and the detector working at 220 nm at a flow rate of 0.5 ml min^{-1}.

2.5 Experimental design and statistical analysis

According to the single factor experiment, the main influencing factors of the SPP-catalyzed sulfoxidation in the water-in-oil microemulsion were determined. Three factors Wo, the concentration of H_2O_2 and the temperature were chosen as independent variables, which are symbolized with A, B, and C, respectively. The conversion rate of substrate the omeprazole thioether was chosen as the dependent variable for the analysis. Using Design Expert 8.0.6, a total of 17 test points were determined by RSM for three factors and three levels, and the central point experiment was conducted 5 times. Table 1 shows these factors and levels.

TABLE 1 Factors and levels of Box-Behnken test design

Factors	Code	Levels		
		-1	0	1
Wo	A	13	16	19
Hydrogen peroxide concentration(mmol/l)	B	17	22	27
Reaction temperature(℃)	C	46	50	54

3 RESULTS AND DISCUSSION

3.1 Enzymatic-catalyzed oxidation of omeprazole sulfide to produce (S)-omeprazole

RSM is a statistical tool widely used for design and analysis of the influence of independent variables on experimental results, determining optimum experimental conditions with the least number of experiments and explore the interactions between independent variables.(Amiri et al., 2019; Selvaraj et al., 2019)

Factors and levels of Box-Behnken test design are shown in Table 1. Table 2 shows the test results of SPP-catalyzed oxidation of the omeprazole sulfide to produce (S)-omeprazole. The optimal fitting model was determined using RSM. Regression analysis was carried out using the Design Expert 8.0.6 package (Table 3) to evaluate the effects of Wo (A), the concentration of hydrogen peroxide (B) and temperature (C) on the conversion rate of the omeprazole thioether. The fitted quadratic polynomial equation was expressed:

$$Y = 93.16-0.37A+0.54B-0.84C+0.47AB+0.43AC-0.50BC-3.86A^2-3.13B^2-5.68C^2 \quad (Y1)$$

TABLE 2 Box–Behnken design and results of RSM

Number	Factor			Conversion rate[a](%)
	A	B	C	
1	0	0	0	93.0
2	1	0	1	82.7
3	1	-1	0	85.1
4	0	1	1	83.8
5	-1	0	1	82.8
6	-1	1	0	86.3
7	0	0	0	93.1
8	0	0	0	92.9
9	1	1	0	86.7
10	0	-1	1	83.3
11	0	0	0	93.1
12	-1	0	-1	85.4
13	0	0	0	93.7
14	-1	-1	0	86.6
15	0	-1	-1	83.9
16	1	0	-1	83.6
17	0	1	-1	86.4

[a] The conversion rate was counted based on a 100% conversion, estimated by HPLC-analysis.

TABLE 3 Analysis of variance and analysis of variance of the fitted model.

Source	Coefficient	Sum of squares	df	Mean squares	F value	p-value
Model		277.10	9	30.79	255.20	<0.0001**
Intercept	93.16		1			
A	-0.37	1.12	1	1.12	9.33	0.0185*
B	0.54	2.31	1	2.31	19.16	0.0032**
C	-0.84	5.61	1	5.61	46.51	0.0002**
AB	0.47	0.90	1	0.90	7.48	0.0291*
AC	0.43	0.72	1	0.72	5.99	0.0443*
BC	-0.50	1.00	1	1.00	8.29	0.0237*
A^2	-3.83	62.57	1	62.57	518.66	< 0.0001**
B^2	-3.13	41.25	1	41.25	341.92	< 0.0001**
C^2	-5.68	135.84	1	135.84	1125.98	< 0.0001**
Residual		0.84	7	0.12		
Lack of Fit		0.45	3	0.15	1.54	0.3347
Pure Error		0.39	4	0.098		
Cor Total		277.94	16			

C.V.%=0.40 R^2 0.9970 R^2_{Adj} 0.9931 R^2_{Pred} 0.9717

*Significant at $p<0.05$. **Significant at $p<0.01$.

A positive coefficient in eq. Y1 means a positive influence on the conversion, on the contrary, a negative coefficient signifies a negative effect on the conversion. As shown in eq. Y1 that B, AB and AC have positive coefficients, implying that these factors favor for the conversion of the omeprazole sulfide. Whereas, all quadratic terms (A^2, B^2 and C^2) and interaction terms (BC) are adverse to the conversion.

The results of analysis of variance are shown in Table 3. As seen in the table 3, the measurement coefficient R^2 was 0.9970, proving that 99.70% of the variation of the conversion can be interpreted by the model, because R^2 of 0.9970 means that the correlation of predicted data with observed is excellent. Furthermore, the adjusted R^2 is 0.9931, implying that the observed results are in good correlation with the predicted. The smaller the p-value (< 0.001), the greater the significance of the corresponding coefficient. On the contrary, the larger the F-value, the greater the significance of the corresponding coefficient. In the present work, the F ratio of the quadratic regression model was 255.20 with a lower probability value ($p < 0.0001$), proving that the model is a very accurate prediction of the conversion. As shown in ANOVA (Table 3) and eq. Y1, the linear influence B, C and all of the quadratic influences have a very significant influence on the conversion ($p < 0.0032$), while the terms of A, AB, AC and BC

were significant at 5 % level ($p < 0.05$). According to the F value, the variable that had the greatest effect on the conversion was the linear term of C. Of all the factors, the reaction temperature (C) had the greatest effect on the conversion that may be because SPP is a biocatalyst with highly sensitivity to reaction temperature. As one of the criteria, with the Prob > F value of the lack-of-fit ($p \geq 0.05$), lack-of-Fit F-value of 1.54 furthermore confirms that the data in the test domain are well expressed by the quadratic polynomial eq. Y1, therefore, which thus is sufficient for simulating the conversion within the range of experimental variables.

3.2 Influence of the interaction of various factors on the conversion of omeprazole sulfide

According to the model, the response surface plots and the contour plots were drawn to seek the best parameters and the interaction between the parameters, which intuitively displays the influence of the interaction between factors on the conversion of the omeprazole sulfide. The results are displayed in Figs.1-3. Each graph has two target variables, and the encoded value of the other variable remains at zero. The effect of Wo (A) and the concentration of hydrogen peroxide (B) on the conversion is shown in FIGURE 1. Wo is the mole ratio of water to CTAB, the effect of Wo on the conversion is showed in FIGURE 1. As shown in FIGURE 1, at the beginning, the conversion increased with the increase of Wo until the maximum conversion, 93.7% with about Wo of 16, appeared, the conversion then decreased with the increase of Wo. There is an optimal Wo which makes the conversion maximum because the size of the water core is suitable for SPP molecules at the optimal Wo. Similarly, the curve shape of the enzyme activity with Wo generally obeys the bell-curve in the microemulsion.(Adachi et al., 2000; Krieger et al., 1997) It is widely believed that the size of the water core plays a key role in affecting enzyme activity which is affected by Wo significantly in the water-in-oil microemulsion,(Carvalho and Cabral, 2000; Chen et al., 2006; Dai and Klibanov, 2000) thus, the conversion is significantly affected by Wo. The optimal Wo signifies that the water core size in the water-in-oil microemulsions is appropriate for the size of the enzyme molecules, resulting in the enzyme exhibiting superactivity. If Wo is very small, the majority of the enzyme molecules cannot be immersed in the water core, but are inactivated directly in organic solvents. Whereas if Wo is larger, the enzyme activity decreases with the increase of Wo, which may be owing to the increase of water content in the microemulsion.(Bru et al.,; Martinek et al., 1989) Figs. 2 and 3 show the interaction between Wo and the temperature, and the interaction between the concentration of hydrogen peroxide and the temperature, respectively. The

reaction temperature had significant influence on the activity and stability of SPP which directly affected the reaction.(Hamann et al., 1997; Schenk et al., 1995) From the graph of temperature to the conversion rate, it could be concluded that the optimal temperature was 49.67 ℃ and the optimal conversion was 93.75% at E_0 of 3200 U ml^{-1}, indicating that SPP has higher thermal stability than HRP because HRP usually works at 20-30 ℃. When the temperature increased continuously after temperature exceed 50 ℃, the conversion decreased gradually, because a high temperature makes SPP inactivation to a certain extent.
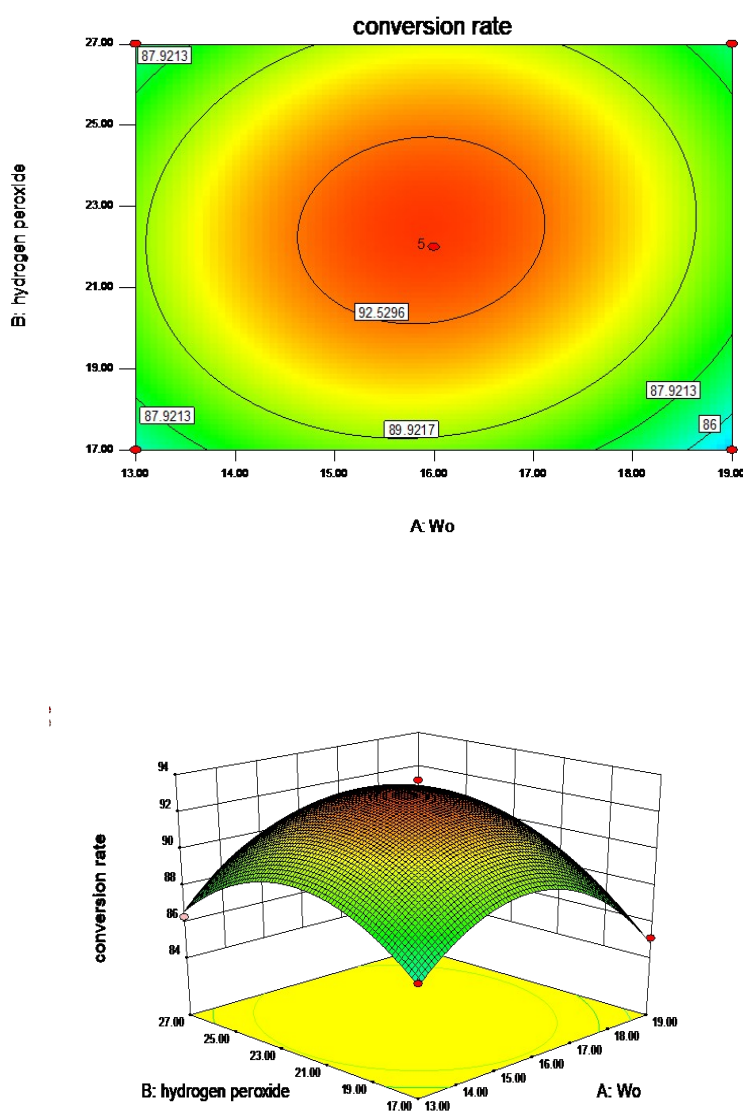
FIGURE 1 Response surface plots and contour plots for the effect of Wo (A) and the concentration of hydrogen peroxide (B) on the conversion rate of the omeprazole sulfide.
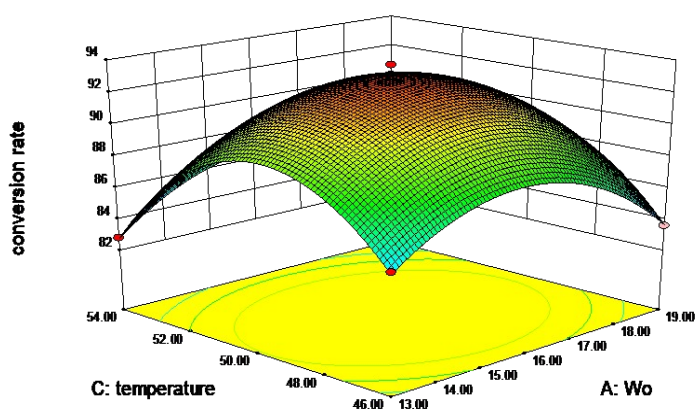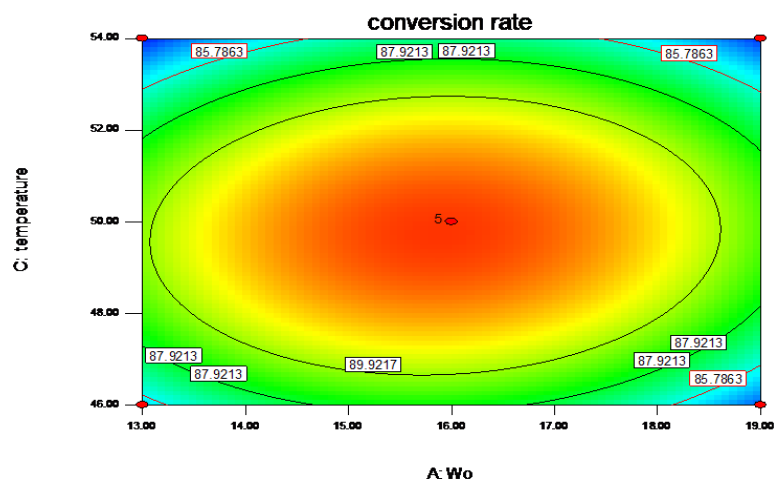
9

FIGURE 2 Response surface plots and contour plots for the effect of Wo (A) and the reaction temperature (C) on the conversion rate of the omeprazole sulfide.
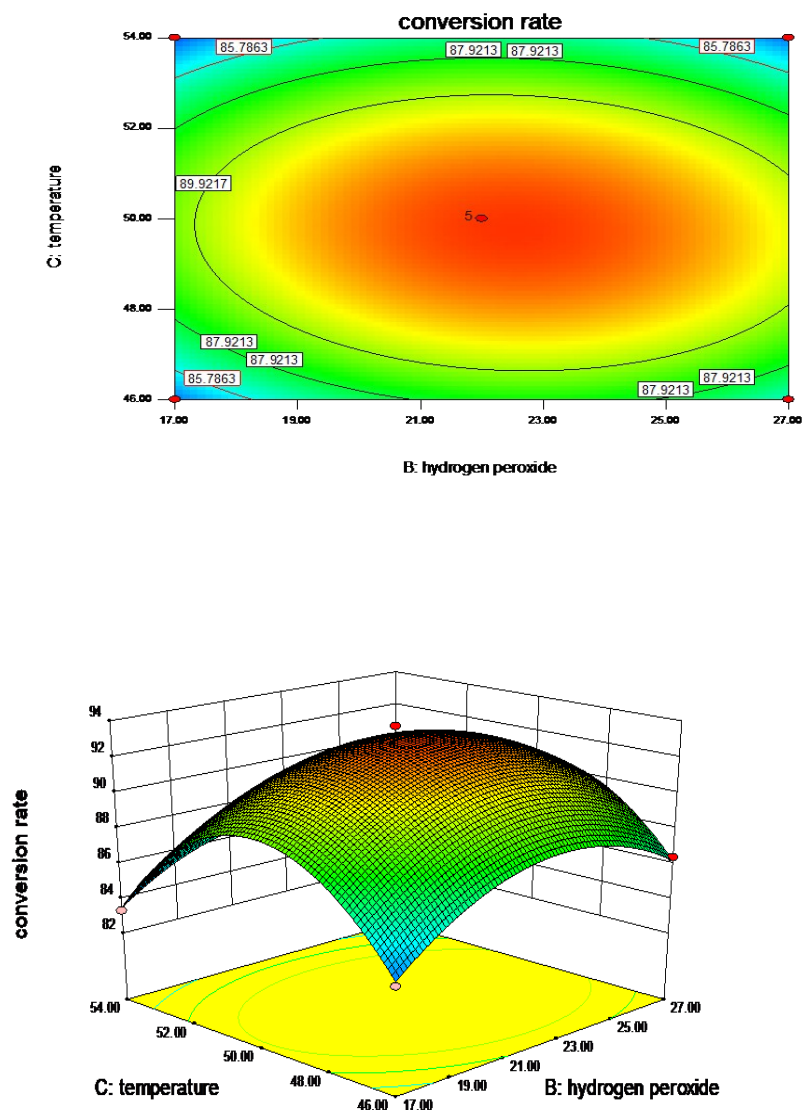
FIGURE 3 Response surface plots and contour plots for the effect of the concentration of hydrogen peroxide (B) and the reaction temperature (C) on the conversion rate of the omeprazole sulfide.

However, the concentration of H_2O_2 had significant effect on the conversion of the oxidation reaction. At the beginning, the conversion rate increased with the increase of the concentration until the concentration reached 22 mM, the omeprazole sulfide: hydrogen peroxide = 1:1.1, the maximum conversion reached 93.75%, then, the conversion decreased as the concentration increased continuously. When the concentration of H_2O_2 was low, H_2O_2 would not match substrate the omeprazole thioether, resulting in decrease of the conversion, when the concentration of H_2O_2 was

large, the SPP activity was partially inhibited, leading to the decrease of conversion because peroxidase can be inactivated by H_2O_2.(Ator et al., 1987; Goodwin et al., 1997) The inactivation appears when enzyme encounters to H_2O_2.(Drożdż et al., 2015) A gradual oxidation process results in disruption of enzyme disulfide bond and loss of protein primary structure.(Katritzky et al., 2003; Törnvall et al., 2009; Törnvall et al., 2010) Therefore, there is a coordinated concentration of H_2O_2 that leads to the conversion maximum (Figs. 1-2). In general, elliptical contour plots mean that the interactions between the corresponding variables are significant, while circular contour plots mean that their interactions are negligible. From the statistical analysis (Table3), the interaction between the concentration of H_2O_2 and the reaction temperature (F value = 8.29) is more meaningful than that of Wo and the concentration of H_2O_2 (F value=7.48). Compared with the above interactions, the interaction between Wo and the reaction temperature was less significant (F value =5.99). The first two have thus greater effect on the conversion than the third, which can be further verified by contour plots (Figs. 1-2).

3.3 Determining and verifying of optimal oxidation conditions

Optimal oxidation conditions were obtained using RSM. Both response surface analysis and contour plots drawn according to the regression equation indicate the effect of Wo, the concentration of hydrogen peroxide and the reaction temperature on the conversion of asymmetric oxidation of the omeprazole thioether catalyzed by SPP in the water-in-oil microemulsion, with which the optimal process was proposed and proved experimentally. The optimal conditions were as follows: Wo value 15.85, the concentration of hydrogen peroxide, 22.44 mM and the reaction temperature, 49.68 ℃, respectively. With three repeated tests at the initial concentration of SPP of 3200 U ml^{-1} and 50 ℃ for 5 h, the conversion rate of the omeprazole sulfide obtained was 93.75%, which was very close to the predicted value (93.23%), and the corresponding (S)-omeprazole yield and ee were 91.56% and 96.08%, respectively, indicating that SPP has excellent enantioselectivity and high thermal stability.

3.4 Kinetic model and sulfoxidation mechanisms

As mentioned earlier the asymmetric sulfoxidations of organic sulfides to form chiral sulfoxides catalyzed by SPP in water-in-oil microemulsions may involve reactions 1-4, however, other three concomitant reactions should also be considered as follows:

$$E_2 + B \rightarrow E + C \qquad (5)$$

$$2C \rightarrow B + R \qquad (6)$$

$$R + Q \rightarrow B + P + 2H^+ \qquad (7)$$
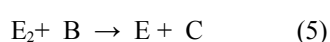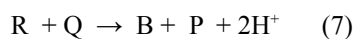
E, E_1 and E_2 are also known as prototype of enzyme, compound I and compound II, and the last two are a transformation form of the prototype(Blake and Coon, 1980; Blee and Schuber, 1989; Ji et al., 2014; Wagner et al., 1983) or $R\text{-}PorFe^{II}$, $R\text{-}^+PorFe^{IV} = O$ and $R\text{-}PorFe^{IV} = O$(Dunford, 1991) and SPP, SPP-I and SPP-II, similar to HRP, HRP-I and HRP-II.(Blee and Schuber, 1989) Many spectroscopic methods have been employed to confirm both HRP-I and II.(Dunford, 1991; Edwards et al., 1987; Fülöp et al., 1994; Harris and Loew, 1996; Samuni et al., 2018) Compound I and II have also been demonstrated by the tests of transient-state kinetics.(Perez and Dunford, 1990)

The reaction mechanism proposed involves seven concomitant reactions. Reactions 1, 2, 3 and 4 were demonstrated by tests in which principal part of ^{18}O, up to 93%, reacting with the sulfoxide, is provided by $H_2^{18}O_2$(Doerge et al., 1991; Hong et al., 2008; Kobayashi et al., 1987; Newmyer and de Montellano, 1995; Perez and Dunford, 1990) and reactions 6 and 7 were proven by tests in which the small amount of ^{18}O from water reacts with thioanisole.(Hashimoto et al., 1986) Reactions 1, and 3-7 were also confirmed by the tests of transient-state kinetics.(Perez and Dunford, 1990) All seven reactions were also confirmed by many spectroscopic methods.(Dunford, 1991; Harris and Loew, 1996; Ji et al., 2014; Samuni et al., 2018)

Using King-Altman method, a kinetic model based on the mechanism was developed which is set of 16 differential equations, such as:

$$dY(1)/dt = -K_{11} \times Y(1) \times Y(2) \times B_0 \times Y(2) \times B_0 \times EK1 \qquad (8)$$

$$dY(2)/dt = -K_{12} \times Y(1) \times A_0 \times Y(2) \times EK1 - K_{13} \times Y(1) \times A_0 \times Y(2) \times B_0 \times Y(2) \times EK2 - K_{14} \times Y(1) \times A_0 \times Y(2) \times EK1 + K_{18} \times (Y(6) \times B_0)^\wedge K19 / B_0 \qquad (9)$$

$$KK1 = K_1 + K_2 \times Y(1) \times A_0 + K_3 \times Y(2) \times B_0 + K_4 \times Y(1) \times A_0 \times Y(2) \times B_0 + K_5 \times Y(1) \times A_0 \times Y(1) \times A_0 + K_6 \times Y(3) \times B_0 + K_7 \times Y(2) \times B_0 \times Y(2) \times B_0 \qquad (10)$$

The proposed mechanisms are as follows: the SPP-catalyzed oxidations including both the two-electron reduction and the single-electron transfer mechanisms should obey ping-pong mechanism with substrate and product inhibition,(Kamble et al., 2016; Mathpati et al., 2016; Zhang et al., 2019c) while nonenzymatic oxidations may follow a power law. Where $K_5 \times Y(1) \times A_0 \times Y(1) \times A_0$ and $K_7 \times Y(2) \times B_0 \times Y(2) \times B_0$ express the substrate inhibition terms of hydrogen peroxide and the omeprazole thioether, respectively, while $K_6 \times Y(3) \times B_0$, the product inhibition term of (S)-omeprazole.

The kinetic model parameters were identified by solving the differential equations integrating optimization for fitting the kinetic model with experimental data by the minimum of the equation 11(Zhang et al., 2019c):

$$F=\sum\sum abs((Y^{simul.}_{ij}-Y^{exp}_{ij}) / Y^{simul.}_{ij}) \qquad (11)$$

The model fits experimental data very well with 5.44% of the average error between simulated data and observed, proving that the mechanism should be reliable and usable, and the parameters are listed in Table 4. The kinetic model can be used to explore the enzymatic reaction process. (Kamble et al., 2016; Mathpati et al., 2016; Zhang et al., 2019b; Zhang et al., 2019c) P_S is the results of concomitant reactions 2, 4 and 7. As shown in FIGURE 4,

TABLE 4 Kinetic parameters estimated.

Parameter	
K_1	0
K_2	32.93
K_3	0.084
K_4	0.0148
K_5	5.68
K_6	435.2
K_7	0.0074
K_8	1.002
K_9	213.036
K_{10}	1.73
K_{11}	0.015
K_{12}	0.0198
K_{13}	0.0056
K_{14}	0.13
K_{15}	1.005
K_{16}	3.45E-07
K_{17}	1.90E-05

the outputs of reactions 2, 4 and 7 are the most, the middle and the least, respectively. The output of reaction 7, in fact, is very small. Similarly, P_R is also contributed by reactions 2, 4 and 7, the contribution of reaction 2, 4 and7 to P_R are the most, the middle and the least, respectively, as shown in FIGURE 5. Comparing Figs. 4 with 5, P_S is far greater than P_R, resulting in a high ee of 96.08% with the yield of P_S of 91.56% and E_0 of 3200 U ml^{-1} (the corresponding concentration of peroxidase was 20 mg U ml^{-1}) (FIGURE 6), thus SPP exhibits excellent enantioselectivity with favoring S configuration in the water-in-oil microemulsion. Therefore, reactions 2 and 4 are the SPP-catalyzed reaction with a

preference for S configuration, whereas reaction 7 is a nonenzymatic reaction with no enantioselectivity. As seen from FIGURE 5, reaction 2 contributes the most to P_S, followed by reaction 4, and reaction 7, a nonenzymatic reaction in fact, contributes the least. Taking enzymatic reactions 2 and 4 into account, we had reason to speculate that the yield of P_S must be further increased if the initial activity of peroxidase is increased. As expected, the yield of P_S increased from 71.98% to 91.56% and e.e decreased slightly from 96.23% to 96.08%, respectively, with the increase of the initial concentration of peroxidase from 960 U ml^{-1} to 3200 U ml^{-1} (the corresponding concentration of peroxidase was 20 mg U ml^{-1}) (FIGURE 6). A higher yield of P_S can thus be obtained if the initial activity of peroxidase is further increased.

Fig. 4 ,3200 Simulated results of PS2, PS4 and PS7
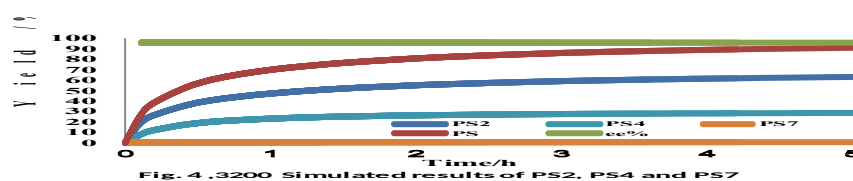
FIGURE 4 The distribution of yield of P_S for reactions 2, 4 and 7, $P_S= P_{S2}+P_{S4}+P_{S7}$
Temperature, 50 °C, stirring speed,150 rpm, E_0=3200 U ml^{-1}, ee (5 h), 96.08%, P_S (5 h), 91.56%, the conversion of the omeprazole sulfide, 93.75%. For E_0=3200 U ml^{-1}, the corresponding concentration of peroxidase was 20 mg U ml^{-1}.
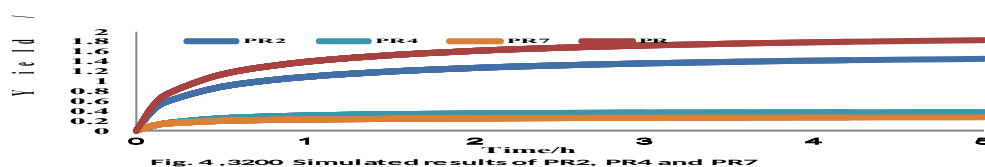
Fig. 4 .3200 Simulated results of PR2, PR4 and PR7

FIGURE 5 The distribution of yield of P_R for reactions 2, 4 and 7, $P_R = P_{R2}+P_{R4}+P_{R7}$
Temperature, 50 °C, stirring speed,150 rpm, E_0=3200 U ml^{-1}, the corresponding concentration of peroxidase, 20 mg U ml^{-1}.
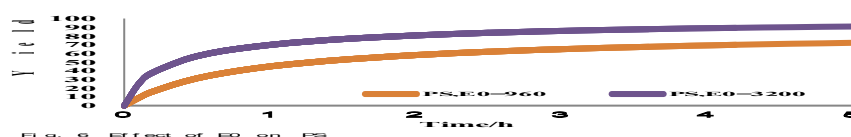

Fig. 6 Effect of E0 on PS

FIGURE 6 Effect of initial activity of peroxidase E_0 on the yield of P_S
Temperature, 50 °C, stirring speed, 150 rpm, ee (5 h), 71.98%, P_S (5 h), 91.56%. For E_0=960 and 3200 U ml^{-1}, the corresponding concentration of peroxidase was 6, and 20 mg U ml^{-1} respectively.

Reaction medium may change the configuration preference of peroxidase. The asymmetric oxidation of thioamidines catalyzed by SHP favours S configuration in aqueous environment, while R configuration in organic solvents.(Dai and Klibanov, 2000) The configuration preference of SPP was S configuration in the present work in water-in-oil microemulsions where SPP is in aqueous environment rather than organic solvent, so its configuration preference should be the same as that in water. The configuration preference of SPP may be different from single water or organic solvents due to the microemulsion including both water and organic solvents, moreover, there may also be some

16

differences in catalytic performance between SPP and SHP.

The asymmetric oxidation catalyzed by soybean hull sulfoxidase in buffer was carried out to form chiral sulfoxide with the ee about 90%,(Blee and Schuber, 1989) whereas soybean hull sulfoxidase in earlier reports did show no chirality selectivity.(Colonna et al., 1999; Kobayashi et al., 1987) The HRP-catalyzed oxidation exhibited significant enantioselectivity, S configuration is about 5 times more than R configuration at both pH 7.0 and 4.5 with the ee of 60-70%.(Harris et al., 1993)

4 CONCLUSIONS

RSM was used to optimize the oxidation of the omeprazole sulfide to form (S)-omeprazole catalyzed by SPP in CTAB/isooctane/n-butyl alcohol/water water-in-oil microemulsions. With the initial concentration of SPP of 3200 U ml^{-1}, the conversion of the omeprazole sulfide, the (S)-omeprazole yield and ee were 93.75%, 91.56% and 96.08%, respectively, under the optimal conditions with Wo of 15.85, the concentration of H_2O_2 of 22.44 and reaction temperature of 49.68 ℃, respectively. A quadratic polynomial model based on RSM was established, and R^2 was 0.9970, indicating that the model predicts the experimental results with high accuracy.

A conclusion can be proposed with certainty that the mechanism of asymmetric sulfoxidations catalyzed by SPP involves three concomitant mechanisms as follows: (1) a two-electron reduction of SPP-I, (2) a single-electron transfer to SPP-I and (3) nonenzymatic reactions, including five enzymatic and two nonenzymatic reactions, which is reasonable and can express the oxidations. The two-electron reduction mechanism includes reactions 1 and 2, while the single-electron transfer mechanism is composed of reactions 1, 3, 4 and 5, and nonenzymatic reactions consists of reactions 6 and 7. With 5.44% of the average relative error, a kinetic model based on the mechanisms fitting observed data very well was established, and the SPP-catalyzed reactions including both the two-electron reduction and the single-electron transfer mechanisms obey ping-pong mechanism with substrate and product inhibition, while nonenzymatic reactions follow a power law. This study has also demonstrated the feasibility of SPP as a substitute with low cost, excellent enantioselectivity and better thermal stability for HRP with high cost in enzymatic catalyzed reactions for production of various chemicals including chiral sulfoxides.

ACKNOWLEDGEMENTS

NOMENCLATURE

A, hydrogen peroxide

A_0, Initial concentration of hydrogen peroxide, mM

B, 5-methoxy-2-(((4-methoxy-3,5-dimethylpyridin-2-yl)methyl)thio)-1H-benzoimidazole, Omeprazole thioether,

5-methoxy-2-(((4-methoxy-3,5-dimethylpyridin-2-yl)methyl)thio)-1H-benzo[d]imidazole

B_0 , Initial concentration of B, mM

C, Cation radical of B, Omeprazole sulfide cation

E_0, Initial concentration of peroxidase, U ml^{-1}

ee, Enantiomeric excess, %

K_1, K_{10}, K_{19}, Kinetic parameter, dimensionless

K_2, K_3, K_6, Kinetic parameter, mM^{-1}

K_4, K_5, K_7, Kinetic parameter, mM^{-2}

K_8, Kinetic parameter, mM^{-3}

K_9, Kinetic parameter, h^{-1} U^{-1}ml mM^{1-2K10}

K_{12}, K_{14}, K_{16}, Kinetic parameter, h^{-1} U^{-1} ml mM^{-1}

K_{11}, K_{13}, K_{15}, K_{17}, Kinetic parameter, h^{-1} U^{-1} ml mM^{-2}

K_{18}, Kinetic parameter, h^{-1} U^{-1}ml mM^{1-K19}

KK1, KK2, ∑K, sum of Kappa constant, dimensionless

P_R, (R)-enantiomer of P

P_S, (S)-enantiomer of P, esomeprazole

P, 5-Methoxy-2-[(4-methoxy-3,5-dimethylpyridin-2-yl) methylsulfinyl]-1H-benzoimidazole, Omeprazole

Q, H_2O

R, dication radical of B

Y(i), Relative residual or yield of A, B, P_S, P_R, C and R, for i=1-6, respectively, dimensionless

$Ysimul_{ij}$, Simulated residual or yield of A, B, P_S and P_R, for i=1-4, j=1-12, dimensionless

$Yexp_{ij}$, Experimental residual or yield of A, B, P_S and P_R, for i=1-4, j=1-12, dimensionless

T, Time, hour

REFERENCES

Adachi M, Harada M, Katoh S. 2000. Bioaffinity separation of chymotrypsinogen using antigen-antibody reaction in reverse micellar system composed of a nonionic surfactant **4**:149–151.

Adam W, Korb MN, Roschmann KJ, Saha-Möller CR. 1998. Titanium-catalyzed, asymmetric sulfoxidation of alkyl aryl sulfides with optically active hydroperoxides. *J. Org. Chem.* **63**:3423–3428.

Akasaka R, Mashino T, Hirobe M. Cytochrome P450-like Substrate Oxidation Catalyzed by

Cytochrome c and Immobilized Cytochrome c. *Arch. Biochem. Biophys.* **301**:0–360.

Amiri S, Shakeri A, Sohrabi MR, Khalajzadeh S, Ghasemi E. 2019. Optimization of ultrasonic assisted extraction of fatty acids from Aesculus hippocastanum fruit by response surface methodology. *Food Chem.* **271**:762–766.

Ator MA, David SK, Montellano PRO De. 1987. Structure and catalytic mechanism of horseradish peroxidase. Regiospecific meso alkylation of the prosthetic heme group by alkylhydrazines. *J. Biol. Chem.* **262**.

Blake RC, Coon MJ. 1980. On the mechanism of action of cytochrome P-450. Spectral intermediates in the reaction of P-450LM2 with peroxy compounds. *J. Biol. Chem.* **255**:4100–4111.

Blee E, Schuber F. 1989. Mechanism of S-oxidation reactions catalyzed by a soybean hydroperoxide-dependent oxygenase. *Biochemistry* **28**:4962–4967.

Bru R, Sánchez-Ferrer A, García-Carmona F. Kinetic models in reverse micelles. *Biochem. J.* **310**:721–739.

Carreño MC. 1995. Applications of sulfoxides to asymmetric synthesis of biologically active compounds. *Chem. Rev.* **95**:1717–1760.

Carvalho CML, Cabral JMS. 2000. Reverse micelles as reaction media for lipases. *Biochimie* **82**:1063–1085.

Chen N, Fan J-B, Xiang J, Chen J, Liang Y. 2006. Enzymatic hydrolysis of microcrystalline cellulose in reverse micelles. *Biochim. Biophys. Acta (BBA)-Proteins Proteomics* **1764**:1029–1035.

Colonna S, Gaggero N, Richelmi C, Carrea G, Pasta P. 1995. Enantioselective sulfoxidations catalyzed by lactoperoxidase.

Colonna S, Gaggereo N, Carrea G, Pasta P. The microperoxidase-11 catalyzed oxidation of sulfides is enantioselective **35**:9103–9104.

Colonna S, Gaggero N, Manfredi A, Casella L, Gullotti M, Carrea G, Pasta P. 1990. Enantioselective oxidations of sulfides catalyzed by chloroperoxidase. *Biochemistry* **29**:10465–10468.

Colonna S, Gaggero N, Carrea G, Pasta P. 1992a. Horseradish peroxidase catalysed sulfoxidation is enantioselective. *J. Chem. Soc. Chem. Commun.*:357–358.

Colonna S, Gaggero N, Casella L, Carrea G, Pasta P. 1992b. Chloroperoxidase and hydrogen peroxide: An efficient system for enzymatic enantioselective sulfoxidations. *Tetrahedron: Asymmetry* **3**:95–106.

Colonna S, Gaggero N, Richelmi C, Pasta P. 1999. Recent biotechnological developments in the use of peroxidases. *Trends Biotechnol.* **17**:163–168.

Dai L, Klibanov AM. 2000. Peroxidase-catalyzed asymmetric sulfoxidation in organic solvents versus in water. *Biotechnol. Bioeng.* **70**:353–357.

Delamare M, Belot S, Caille J-C, Martinet F, Kagan HB, Henryon V. 2009. A new titanate/(+)-(1R, 2S)-cis-1-amino-2-indanol system for the asymmetric synthesis of (S)-tenatoprazole. *Tetrahedron Lett.* **50**:1702–1704.

Dembitsky VM. 2003. Oxidation, epoxidation and sulfoxidation reactions catalysed by haloperoxidases. *Tetrahedron* **26**:4701–4720.

Van Deurzen MPJ, van Rantwijk F, Sheldon RA. 1997. Selective oxidations catalyzed by peroxidases. *Tetrahedron* **53**:13183–13220.

Doerge DR. 1986. Oxygenation of organosulfur compounds by peroxidases: evidence of an electron transfer mechanism for lactoperoxidase. *Arch. Biochem. Biophys.* **244**:678–685.

Doerge DR, Cooray NM, Brewster ME. 1991. Peroxidase-catalyzed S-oxygenation: mechanism of

oxygen transfer for lactoperoxidase. *Biochemistry* **30**:8960–8964.

Drożdż A, Erfurt K, Bielas R, Chrobok A. 2015. Chemo-enzymatic Baeyer–Villiger oxidation in the presence of Candida antarctica lipase B and ionic liquids. *New J. Chem.* **39**:1315–1321.

Dunford HB. 1991. Horseradish peroxidase: structure and kinetic properties. *Perozidases Chem. Biol.*:1–23.

Edwards SL, Xuong NH, Hamlin RC, Kraut J. 1987. Crystal structure of cytochrome c peroxidase compound I. *Biochemistry* **26**:1503–1511.

Federsel HJ. Process R&D under the magnifying glass: Organization, business model, challenges, and scientific context **18**:5775–5794.

Fülöp V, Phizackerley RP, Soltis SM, Clifton IJ, Wakatsuki S, Erman J, Hajdu J, Edwards SL. 1994. Laue diffraction study on the structure of cytochrome c peroxidase compound I. *Structure* **2**:201–208.

Goodwin DC, Grover TA, Aust SD. 1997. Roles of efficient substrates in enhancement of peroxidase-catalyzed oxidations. *Biochemistry* **36**:139–147.

Hamann H-J, Höft E, Mostowicz D, Mishnev A, Urbańczyk-Lipkowska Z, Chmielewski M. 1997. New optically pure sugar hydroperoxides. Synhtesis and use for enantioselective oxygen transfer. *Tetrahedron* **53**:185–192.

Harris DL, Loew GH. 1996. Identification of putative peroxide intermediates of peroxidases by electronic structure and spectra calculations. *J. Am. Chem. Soc.* **118**:10588–10594.

Harris RZ, Newmyer SL, De Montellano PRO. 1993. Horseradish peroxidase-catalyzed two-electron oxidations. Oxidation of iodide, thioanisoles, and phenols at distinct sites. *J. Biol. Chem.* **268**:1637–1645.

Hashimoto S, Tatsuno Y, Kitagawa T. 1986. Resonance Raman evidence for oxygen exchange between the FeIV= O heme and bulk water during enzymic catalysis of horseradish peroxidase and its relation with the heme-linked ionization. *Proc. Natl. Acad. Sci.* **83**:2417–2421.

Hong ES, Kwon OY, Ryu K. 2008. Strong substrate-stabilizing effect of a water-miscible ionic liquid [BMIM][BF 4] in the catalysis of horseradish peroxidase. *Biotechnol. Lett.* **30**:529–533.

Ji L, Franke A, Brindell M, Oszajca M, Zahl A, van Eldik R. 2014. Combined experimental and theoretical study on the reactivity of Compounds I and II in horseradish peroxidase biomimetics. *Chem. Eur. J.* **20**:14437–14450.

Kamble MP, Shinde SD, Yadav GD. 2016. Kinetic resolution of (R, S)-α-tetralol catalyzed by crosslinked Candida antarctica lipase B enzyme supported on mesocellular foam: a nanoscale enzyme reactor approach. *J. Mol. Catal. B Enzym.* **132**:61–66.

Kamerbeek NM, Olsthoorn AJJ, Fraaije MW, Janssen DB. Substrate Specificity and Enantioselectivity of 4-Hydroxyacetophenone Monooxygenase. *Appl. Environ. Microbiol.* **69**:419–426.

Katritzky AR, Akhmedov NG, Denisko O V. 2003. 1H and 13C NMR spectroscopic study of oxidation of d, l-cystine and 3, 3′-dithiobis (propionic acid) with hydrogen peroxide in aqueous solution. *Magn. Reson. Chem.* **41**:37–41.

Kobayashi S, Nakano M, Kimura T, Schaap AP. 1987. On the mechanism of the peroxidase-catalyzed oxygen-transfer reaction. *Biochemistry* **26**:5019–5022.

Krieger N, Taipa MA, Melo EHM, Lima-Filho JL, Aires-Barros MR, Cabral JMS. 1997. Kinetic characterization ofpenicillium citrinum lipase in AOT/lsooctane-reversed micelles. *Appl. Biochem. Biotechnol.* **67**:87–95.

Lee Y-M, Kwon O-Y, Yoo I-K, Ryu K-G. 2007. Effect of ionic liquid on the kinetics of peroxidase

catalysis. *J. Microbiol. Biotechnol.* **17**:600–603.

Li AT, Yu H-L, Pan J, Zhang J-D, Xu J-H, Lin G-Q. Resolution of racemic sulfoxides with high productivity and enantioselectivity by a Rhodococcus sp. strain as an alternative to biooxidation of prochiral sulfides for efficient production of enantiopure sulfoxides **102**:1537–1542.

Lopez F, Palazzo G, Colafemmina G, Cinelli G, Ambrosone L, Ceglie A. 2004. Enzymatic activity of lipase entrapped in CTAB/water/pentanol/hexane reverse micelles: a functional and microstructural investigation **123**:174–177.

Lopez F, Cinelli G, Ambrosone L, Colafemmina G, Ceglie A, Palazzo G. Role of the cosurfactant in water-in-oil microemulsion: interfacial properties tune the enzymatic activity of lipase **237**:49–59.

Lopez F, Cinelli G, Colella M, De Leonardis A, Palazzo G, Ambrosone L. 2014. The role of microemulsions in lipase-catalyzed hydrolysis reactions. *Biotechnol. Prog.* **30**:360–366.

Martinek K, Klyachko NL, Kabanov A V, Khmelnitsky YL, Levashov A V. 1989. Micellar enzymology: Its relation to membranology. *Biochim. Biophys. Acta - Biomembr.* **981**:161–172.

Mathpati AC, Badgujar KC, Bhanage BM. 2016. Kinetic modeling and docking study of immobilized lipase catalyzed synthesis of furfuryl acetate. *Enzyme Microb. Technol.* **84**:1–10.

Miller VP, DePillis GD, Ferrer JC, Mauk AG, De Montellano PRO. 1992. Monooxygenase activity of cytochrome c peroxidase. *J. Biol. Chem.* **267**:8936–8942.

Newmyer SL, de Montellano PRO. 1995. Horseradish Peroxidase His-42→ Ala, His-42→ Val, and Phe-41→ Ala Mutants HISTIDINE CATALYSIS AND CONTROL OF SUBSTRATE ACCESS TO THE HEME IRON. *J. Biol. Chem.* **270**:19430–19438.

Ortiz de Montellano PR. 1987. Control of the catalytic activity of prosthetic heme by the structure of hemoproteins. *Acc. Chem. Res.* **20**:289–294.

Ozaki SI, Matsui T, Watanabe Y. Conversion of Myoglobin into a Peroxygenase:? A Catalytic Intermediate of Sulfoxidation and Epoxidation by the F43H/H64L Mutant. *J. Am. Chem. Soc.* **119**:6666–6667.

Ozaki SI, Yang HJ, Matsui T, Goto Y, Watanabe Y. 1999. Asymmetric Oxidation Catalyzed by Myoglobin Mutants. *Tetrahedron Asymmetry* **10**:183–192.

Perez U, Dunford HB. 1990. Transient-state kinetics of the reactions of 1-methoxy-4-(methylthio) benzene with horseradish peroxidase compounds I and II. *Biochemistry* **29**:2757–2763.

Prasad KD. 2001. Intermediates and an improved process for the preparation of omeprazole employing the said intermediates. Google Patents.

Samuni U, Maimon E, Goldstein S. 2018. A kinetic study of the oxidation of hydroxamic acids by compounds I and II of horseradish peroxidase: Effect of transition metal ions. *J. Coord. Chem.* **71**:1728–1737.

Schenk WA, Frisch J, Adam W, Prechtl F. 1995. Sulfur (IV) Compounds as Ligands. Part 21. Oxidation of Metal-Coordinated Thioethers with Dimethyldioxirane. A New Stereoselective Synthesis of Chiral Sulfoxides. *ChemInform* **26**:no-no.

Seenivasaperumal M, Federsel H-J, Szab K. 2010. Mechanism of the Asymmetric Sulfoxidation in the Esomeprazole Process: Effects of the Imidazole Backbone for the Enantioselection. *Adv. Synth. Catal.* **351**:903–919.

Selvaraj R, Moorthy IG, Kumar RV, Sivasubramanian V. 2019. Microwave mediated production of FAME from waste cooking oil: Modelling and optimization of process parameters by RSM and ANN approach. *Fuel* **237**:40–49.

Singh P, Prakash R, Shah K. 2012. Effect of organic solvents on peroxidases from rice and horseradish: prospects for enzyme based applications. *Talanta* **97**:204–210.

Thomas SM, DiCosimo R, Nagarajan V. 2002. Biocatalysis: applications and potentials for the chemical industry. *TRENDS Biotechnol.* **20**:238–242.

Törnvall U, Fürst CM, Hatti-Kaul R, Hedström M. 2009. Mass spectrometric analysis of peptides from an immobilized lipase: focus on oxidative modifications. *Rapid Commun. Mass Spectrom. An Int. J. Devoted to Rapid Dissem. Up-to-the-Minute Res. Mass Spectrom.* **23**:2959–2964.

Törnvall U, Hedström M, Schillén K, Hatti-Kaul R. 2010. Structural, functional and chemical changes in Pseudozyma antarctica lipase B on exposure to hydrogen peroxide. *Biochimie* **92**:1867–1875.

van de Velde F, Könemann L, van Rantwijk F, Sheldon RA. 2000. The rational design of semisynthetic peroxidases. *Biotechnol. Bioeng.* **67**:87–96.

Wagner GC, Palcic MM, Dunford HB. 1983. Absorption spectra of cytochrome P450CAM in the reaction with peroxy acids. *FEBS Lett.* **156**:244–248.

Watanabe Y, Iyanagi T, Oae S. 1980. Kinetic study on enzymatic S-oxygenation promoted by a reconstituted system with purified cytochrome P-450. *Tetrahedron Lett.* **21**:3685–3688.

Zambianchi F, Fraaije MW, Carrea G, de Gonzalo G, Rodríguez C, Gotor V, Ottolina G. 2007. Titration and assignment of residues that regulate the enantioselectivity of phenylacetone monooxygenase. *Adv. Synth. Catal.* **349**:1327–1331.

Zhang Y, Liu F, Xu N, Wu Y-Q, Zheng Y-C, Zhao Q, Lin G, Yu H-L, Xu J-H. 2018. Discovery of two native Baeyer-Villiger monooxygenases for asymmetric synthesis of bulky chiral sulfoxides. *Appl. Environ. Microbiol.* **84**:e00638-18.

Zhang Y, Wu Y-Q, Xu N, Zhao Q, Yu H-L, Xu J-H. 2019a. Engineering of cyclohexanone monooxygenase for the enantioselective synthesis of (S)-omeprazole. *ACS Sustain. Chem. Eng.* **7**:7218–7226.

Zhang Y, Zhao Y, Gao X, Jiang W, Li Z, Yao Q, Yang F, Wang F, Liu J. 2019b. Kinetic model of the enzymatic Michael addition for synthesis of mitomycin analogs catalyzed by immobilized lipase from T. laibacchii. *Mol. Catal.* **466**:146–156.

Zhang Y, Zhao Y, Jiang W, Yao Q, Li Z, Gao X, Liu T, Yang F, Wang F, Liu J. 2019c. Lipase-catalyzed oxidation of cyclohexanone to form ε-caprolactone and kinetic modeling. *ACS Sustain. Chem. Eng.* **7**:13294–13306.

Table legend
Table 1 Factors and levels of Box-Behnken test design

Table 2 Box–Behnken design and results of RSM

Table 3 Analysis of variance and analysis of variance of the fitted model

Table 4 Kinetic Parameters Estimated.

Figure legend

FIGURE 1 Response surface plots and contour plots for the effect of Wo (A) and the concentration of hydrogen peroxide (B) on the conversion rate of the omeprazole sulfide .

FIGURE 2 Response surface plots and contour plots for the effect of Wo value(A) and the reaction temperature (C) on the conversion rate of the omeprazole sulfide.

FIGURE 3 Response surface plots and contour plots for the effect of the concentration of hydrogen peroxide (B) and the reaction temperature (C) on the conversion rate of the omeprazole sulfide.

FIGURE 4 The distribution of yield of P_S for reactions 2, 4 and 7, $P_S = P_{S2} + P_{S4} + P_{S7}$
Temperature, 50°C, stirring speed,150 rpm, $E_0 = 3200$ U ml^{-1}, ee (5 h), 96.08%, P_S (5 h), 91.56%, the conversion of the omeprazole sulfide, 93.75%. For $E_0 = 3200$ U ml^{-1}, the corresponding concentration of peroxidase was 20 mg U ml^{-1}.

FIGURE 5 The distribution of yield of P_R for reactions 2, 4 and 7, $P_R = P_{R2} + P_{R4} + P_{R7}$
Temperature, 50°C, stirring speed,150 rpm, $E_0 = 3200$ U ml^{-1}, the corresponding concentration of peroxidase, 20 mg U ml^{-1}.

FIGURE 6 Effect of initial activity of peroxidase E_0 on the yield of P_S
Temperature, 50°C, stirring speed, 150 rpm, ee (5 h), 96.08%, P_S (5 h), 91.56%. For $E_0 = 960$ and 3200 U ml^{-1}, the corresponding concentration of peroxidase was 6, and 20 mg U ml^{-1} respectively.